

Reactivity of (*E*)-4-aryl-4-oxo-2-butenic acid phenylamides with piperidine and benzylamine: kinetic and theoretical study

Ilija N. Cvijetić · Maja D. Vitorović-Todorović · Ivan O. Juranić ·
Đura J. Nakarada · Milica D. Milosavljević · Branko J. Drakulić

Received: 17 January 2014 / Accepted: 3 April 2014 / Published online: 28 May 2014
© Springer-Verlag Wien 2014

Abstract Rates of the aza-Michael addition of piperidine and benzylamine to thirteen (*E*)-4-aryl-4-oxo-2-butenic acid phenylamides (AACP)s are reported. Progress of the reaction was monitored by UV/Vis spectroscopy. The 2D NMR spectra confirmed regioselectivity of the reactions. Piperidine and benzylamine provide exclusively β -adducts in respect to the aroyl keto group. Influence of the substituents of the aroyl phenyl ring of AACPs on the rate of the reaction was quantified by Hammett substituent constants, partial atomic charges, and the energies of frontier orbitals. Good correlations between second-order rate constants and the Hammett substituent constants were obtained ($r = 0.98$, piperidine; $r = 0.94$, benzylamine) for *para*-, and *meta*-, *para*-substituted derivatives. Best correlations were obtained with the energies of the lowest unoccupied molecular

orbitals of compounds, derived from the MP2 level of theory. Calculated UV/Vis spectra of representative AACPs and their Michael adduct with piperidine and benzylamine are in fair agreement with experimentally obtained data.

Keywords Michael addition · UV/Vis spectroscopy · Kinetics · Linear free-energy relationships · ZINDO/S calculations

Introduction

Recently, we showed that (*E*)-4-aryl-4-oxo-2-butenic acid amides exert antiproliferative activity toward human tumor cell lines in submicromolar to low micromolar concentrations in vitro. Some of derivatives act as inhibitors of tubulin polymerization [1]. Michael adducts of cyclic amines and (*E*)-4-aryl-4-oxo-2-butenic acid amides (AACPs) are micromolar acetyl- and butyrylcholinesterase inhibitors [2]. We previously examined reactivity of title compounds with thiols, using 2-mercaptoethanol as a model nucleophile [3], and observed a correlation between the rate constants of addition and the nature of substituents on aroyl and phenylamido moieties.

The Michael addition of compounds containing a heteroatom as a nucleophile to the activated double bonds has been known for almost 150 years. First addition of amines to the alkenes activated by electron-withdrawing groups (aza-Michael reaction) was reported in 1874 [4]. Reaction leads to the β -amino carbonyl compounds (β -lactams, β -amino acids etc.) [5–7], important bioactive compounds and useful synthetic precursors. Very good coverage of aza-Michael additions can be found in recent review articles [8, 9].

Electronic supplementary material The online version of this article (doi:10.1007/s00706-014-1223-8) contains supplementary material, which is available to authorized users.

I. N. Cvijetić (✉)
Innovation Center of the Faculty of Chemistry, University of
Belgrade, Studentski Trg 12-16, Belgrade, Serbia
e-mail: ilija@chem.bg.ac.rs

M. D. Vitorović-Todorović
Military - Technical Institute, Ratka Resanovića 1,
Belgrade, Serbia

I. O. Juranić · B. J. Drakulić (✉)
Department of Chemistry-ICHM, University of Belgrade,
Njegoševa 12, Belgrade, Serbia
e-mail: bdrakuli@chem.bg.ac.rs

Đ. J. Nakarada · M. D. Milosavljević
Faculty of Chemistry, University of Belgrade, Studentski Trg
12-16, Belgrade, Serbia

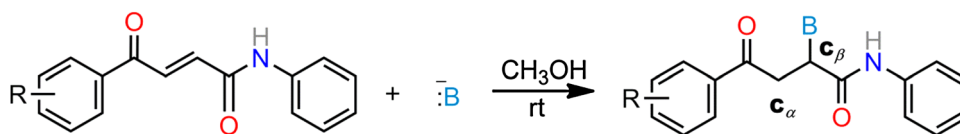


Fig. 1 Michael addition of deprotonated piperidine or benzylamine (abbreviated as B^-) to compounds **1–13**. R = **1** H; **2** 4-*i*-Pr; **3** 4-*n*-Bu; **4** 4-*tert*-Bu; **5** 3,4-di-Me; **6** 2,5-di-Me; **7** 2,4-di-*i*-Pr; **8** β -tetralinyl; **9** 4-OMe; **10** 4-F; **11** 4-Cl; **12** 4-Br; **13** 3,4-di-Cl

Within the frame of toxicity prediction, as the alternative methods to animal testing, the aza-Michael additions were proved to be a useful tool. Relative Alkylation Index [10] was developed for quantification of the alkylation potency of chemicals. In this approach, the relative rate of adduct formation with *n*-butylamine have been used for the estimation of reactivity of a given chemical.

In this study, we used UV/Vis spectroscopy to examine the rate of addition of piperidine and benzylamine as models of secondary and primary amine, respectively, to title compounds.

Results and discussion

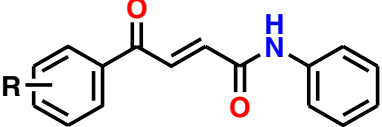
The rates of addition of piperidine and benzylamine to compounds **1–13** (Fig. 1) in methanol were examined by UV/Vis spectrophotometry.

The UV/Vis spectra of compound **1**, recorded before time scan measurements, and of adducts of compound **1** with piperidine and with benzylamine, recorded at the end of time scan measurements, are given in Supplementary Material, Fig. S1. Spectra of representative AACPs and adducts with piperidine and benzylamine are shown in Supplementary Material, Figs. S2 and S3.

We observed that addition does not proceed in aprotic solvent. In CCl_4 , there was no change in UV/Vis spectra of compound **1**, 24 h after the addition of amines. Changing the solvent to methanol, we observed the alterations in UV/Vis spectra upon the addition of amine, but the reaction was very slow. Any observable decrease of the peak intensity in UV/Vis spectra at ~ 310 nm appears only after several hours, at room temperature. Significant acceleration of the reaction was achieved by using the deprotonated amines.

The UV/Vis spectra of the adducts of piperidine and benzylamine and compounds **1–13** lack the absorption maximum at ~ 310 nm, which appears in the UV/Vis spectra of **1–13**, and corresponds to the conjugated double bond chromophore. On the other hand, the peak at ~ 260 nm appears in the UV/Vis spectra of adducts (Figs. S1, S2, and S3). In previous work [3], we monitored the progress of the reaction at two wavelengths simultaneously, through decrease of absorbance at ~ 310 nm and increase of absorbance at ~ 260 nm. Obtained rate

Table 1 Rate constants (k_2) of the addition of piperidine and benzylamine to compounds **1–13** and Hammett σ constants



Comp. N°	R-	Hammett σ	$k_2 \times 10^{-5}/\text{dm}^3 \text{ mol}^{-1} \text{ s}^{-1}$	
			Piperidine	Benzylamine
1	H	0	9.86 (± 0.59)	6.80 (± 0.25)
2	4- <i>i</i> -C ₃ H ₇	−0.15	5.70 (± 0.25)	3.32 (± 0.09)
3	4- <i>n</i> -C ₄ H ₉	−0.16	5.44 (± 0.26)	3.57 (± 0.17)
4	4- <i>tert</i> -C ₄ H ₉	−0.20	5.27 (± 0.34)	3.83 (± 0.18)
5	3,4-di-CH ₃	−0.30	6.29 (± 0.42)	4.00 (± 0.17)
6	2,5-di-CH ₃	–	9.18 (± 0.85)	5.87 (± 0.21)
7	2,4-di- <i>i</i> -C ₃ H ₇	–	4.85 (± 0.09)	4.51 (± 0.25)
8	β -tetralinyl	−0.48	5.44 (± 0.42)	3.83 (± 0.23)
9	4-OCH ₃	−0.78	2.98 (± 0.17)	1.96 (± 0.08)
10	4-F	0.06	12.92 (± 0.93)	9.01 (± 0.34)
11	4-Cl	0.23	17.43 (± 1.27)	10.63 (± 0.60)
12	4-Br	0.23	15.64 (± 1.02)	11.14 (± 0.51)
13	3,4-di-Cl	0.52	28.65 (± 2.29)	15.64 (± 0.94)

constants were the same. In this study, we monitored the rate of addition of amines at a wavelength of ~ 310 nm. A detailed description of the determination of rate constants is given in the Experimental section. Results are shown in Table 1. The difference in reactivity among studied compounds is illustrated by the time scan plots, given in Fig. S4 in Supplementary Material.

The rate constants for the addition of piperidine to AACPs are higher than corresponding rate constants for the addition of benzylamine. Although piperidine ($\text{p}K_a = 11.01$ [11]) is a stronger base than benzylamine ($\text{p}K_a = 8.52$ [12]), higher rate constants for the addition of piperidine could not be ascribed solely to the basicity of amines. While there is a poor correlation between basicity and nucleophilicity of amines, for example, see Ref. [13], piperidine is also more nucleophilic than benzylamine. Nucleophilicity parameters, N , determined by the reactivity toward benzhydrylium cations as a referent electrophile for

piperidine and benzylamine are 15.63 and 13.46, respectively [14]. So, higher rate constants of the addition of piperidine to title compounds, compared to benzylamine, could be ascribed to higher nucleophilicity of the former.

The second order rate constants for the addition of 2-mercaptoethanol to compounds **1–13** [3] were one to two orders of magnitude higher than the values for piperidine and benzylamine. Consequently, in studied reactions, thiols (as the soft bases) are more efficient Michael donors than amines.

Linear free energy relationship (LFER)

The LFER correlates in a quantitative manner to the equilibrium, or rate constants of two different reactions of the same or the analogous set of compounds. Hammett type correlations, as a one of implementations of the LFER principle, are widely used for quantification of the influence of structural changes on the reactivity in congeneric sets of compounds; see, for example, references [15, 16].

During the experiments, we observed that the time scan plots are influenced by the nature of the substituents on the aryl ring. The effects of aryl ring substitution on the rate of reaction for compounds **1–5**, **8–13** were quantified by using the Hammett approach, Eq. (1) [17]:

$$\log \left(\frac{k_R}{k_H} \right) = \rho \times \sigma, \quad (1)$$

where σ is substituent constant, ρ is reaction constant, k_R is the rate constant for the *meta*- or *para*-substituted derivative, and k_H is the rate constant for the unsubstituted compound **1**. Hammett plots are shown in Fig. 2.

Compounds **6** and **7**, the only AACPs with *ortho*-alkyl substituents, were excluded from the correlations shown in Fig. 2. Along with electronic effects, substituents in the *ortho*-position exert steric effects. More detailed discussion on the exclusion of *ortho*-substituted congeners, in the similar set of compounds, was given in a previous article [3]. Briefly, Ar–C(O) torsion in the aryl part of molecule is much larger for derivatives **6** and **7**, compared to other compounds, due to steric repulsion between the *ortho*-alkyl substituent and the aryl keto group. As a consequence, the conjugation of aryl moiety with the α,β -unsaturated carbonyl group is attenuated. For the *p*-OCH₃ derivative (compound **9**), σ^+ value (−0.78) fits much better to the correlations than σ (−0.27), most probably because of hyperconjugation of the *p*-OCH₃ group through the whole molecule. In the examined set, such effect can be proposed only for compound **9**.

The reaction constant, ρ , was calculated as a slope of the best-fit line, obtained by plotting numerical values of the rate constants of addition against σ constants. It reflects the relative sensitivity of a particular reaction on the variation of substituents on the aromatic ring. The reaction constant is very sensitive to the reaction conditions. The sign and the magnitude of the reaction constant are strongly influenced by the nature of the reactants and the mechanism of reaction. Positive signs of reaction constants for the addition of piperidine and benzylamine ($\rho = 0.89$ and $\rho = 0.75$, respectively) to AACPs indicate that electron-withdrawing substituents increase the rate of addition. Numerical values of the reaction constants indicate the formation of the charged species in the rate-limiting step, which is in accordance with proposed mechanism of the

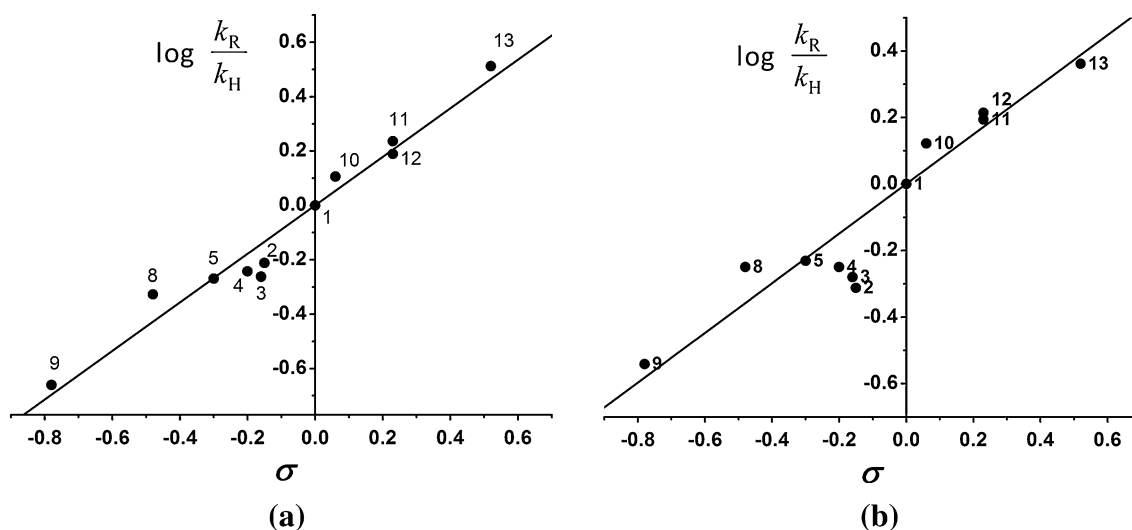


Fig. 2 Plot of the rate constants versus Hammett substituent constants for compounds **1–5**, **8–13**; **a** Addition of piperidine, $r = 0.981$, $n = 11$, $F = 219.1$, $\rho = 0.89$ (± 0.06); **b** Addition of

benzylamine, $r = 0.938$, $n = 11$, $F = 66.4$, $\rho = 0.75$ (± 0.09). Compounds **6** and **7** are omitted from the correlations

formation of carbanionic intermediate and its subsequent rapid protonation in aza-Michael additions [18]. Polar solvents, capable of stabilizing charged species in the transition state, lead to the formation of adduct. The absence of adducts formation in CCl_4 is in line with the existence of polar/charged intermediates in the reaction mechanism.

Along with correlations with Hammett substituent constants, we derived correlations employing descriptors obtained from geometries of molecules fully optimized on the MP2 level of theory. The MP2 method seems to be good for geometry optimizations of studied structures. Limitations of other methods tested for geometry optimization of title compounds (semiempirical and DFT) were described in a previous study [3]. Mulliken atomic charges on C_β atom and energies of Highest Occupied Molecular Orbital (HOMO) and Lowest Unoccupied Molecular Orbital (LUMO) orbitals, derived from MP2 calculations in the ground state of molecules, are given in Table 2.

Correlations of the second order rate constants for the addition of piperidine and benzylamine and the Mulliken atomic charges of the reaction center, with carbon in the β -position in respect to the aroyl keto group, are shown

Table 2 Mulliken charges on C_β , and energies of HOMO and LUMO for compounds 1–13, as obtained from calculations in vacuo

Comp. N°	Mulliken charge $\text{C}_\beta/\text{a.u.}$	$E_{\text{HOMO}}/\text{Hartree}$	$E_{\text{LUMO}}/\text{Hartree}$	μ/Debye
1	−0.2353	−0.3214 −0.3211 ^a	0.0212 0.0194 ^a	0.8119 0.9584 ^a
2	−0.2362	−0.3204	0.0243	–
3	−0.2386	−0.3201	0.0246	–
4	−0.2363	−0.3203	0.0245	–
5	−0.2372	−0.3199	0.0250	–
6	−0.2235	−0.3207 −0.3210 ^a	0.0232 0.0201 ^a	0.9225 1.3383 ^a
7	−0.2238	−0.3205	0.0250	–
8	−0.2372	−0.3197	0.0254	–
9	−0.2372	−0.3203	0.0247	–
10	−0.2296	−0.3250	0.0137	–
11	−0.2293	−0.3253	0.0113	–
12	−0.2302	−0.3245	0.0127	–
13	−0.2252	−0.3281	0.0033	–
1a	–	−0.3072 −0.3159 ^a	0.0778 0.0682 ^a	5.1513 7.0073 ^a
6a	–	−0.3066 −0.3169 ^a	0.0569 0.0629 ^a	4.9584 5.8870 ^a

HOMO, LUMO, and dipole moments of compounds 1, 6, 1a, and 6a are reported for geometries optimized in vacuo, and by using implicit solvent model (CH_3OH)

^a Obtained using implicit solvent model

in Supplementary Material, Fig. S5. Mulliken atomic charges of C_β atom are well correlated with experimentally determined rate constants. The substituent effects are transmitted from the aroyl ring to the C_β atom. Compounds 6 and 7 are strong outliers in these correlations.

In the reactions of nucleophilic addition, the LUMO of acceptor is the most probable site of attack of the HOMO of the nucleophile. The LUMO orbital is situated on α,β -unsaturated keto moiety in all AACPs, as exemplified for compounds 1 and 6 (Fig. 3).

Statistically significant correlations between k_2 and the energies of LUMO orbitals were obtained for addition of both piperidine and benzylamine (Fig. 4). The *ortho*-substituted derivatives fit into these correlations, opposite to correlations obtained with the atomic charges on C_β and Hammett σ constants.

Correlations between the rate constants for addition of piperidine and benzylamine and the atomic charges on C_β , or the energies of LUMO orbitals, shown in Fig. S5 and Fig. 4, were obtained from the geometry of the molecules optimized on the MP2 level of theory, without an applied solvent model (in vacuo). Since we measured the rate constants of the addition in methanol as a solvent, the charge distribution of molecules is recalculated using an implicit solvent model (PCM-methanol). Correlations between the rate constants for the addition of piperidine and benzylamine and the atomic charges on C_β and the energies of LUMO, are calculated with the applied implicit solvent model, and are shown in Supplementary Material, Fig. S6 and S7. Correlations with atomic charges on C_β were slightly improved, while correlations with energies of LUMO orbitals appeared similar to the correlations obtained from calculations in which the solvation effect were not considered. In all correlations where the implicit solvent model was used, compound 10 appears as a strong outlier, most probably implying an over-estimated polarizability of fluorine.

Regioselectivity

Addition of piperidine and benzylamine to (*E*)-4-aryl-4-oxo-2-butenic acid phenyamides produced stable addition products. So far, we isolated a number of adducts of piperidine to AACPs [2]. Along with this, we isolated and characterized an adduct of benzylamine to derivative 6. AACPs comprise a double bond bound to the aroyl (ArC(O)-) and the phenylamido moieties (PhNH-C(O)-), both of which are electron-withdrawing. Each moiety could activate a corresponding C_β carbon of the double bond for nucleophilic addition. To confirm regioselectivity of the addition, we recorded NOESY spectra of adducts of piperidine and benzylamine to compound 6. In the

Fig. 3 **a** HOMO orbital of compound **1**; **b** LUMO orbital of compound **1**; **c** HOMO orbital of compound **6**; **d** LUMO orbital of compound **6**. Major parts of LUMO orbitals are located on the Michael acceptor moiety of the molecules. Depicted orbitals are obtained by MP2 calculations

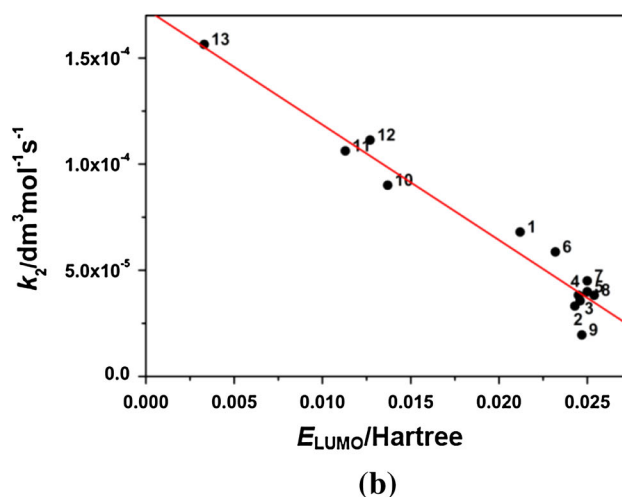
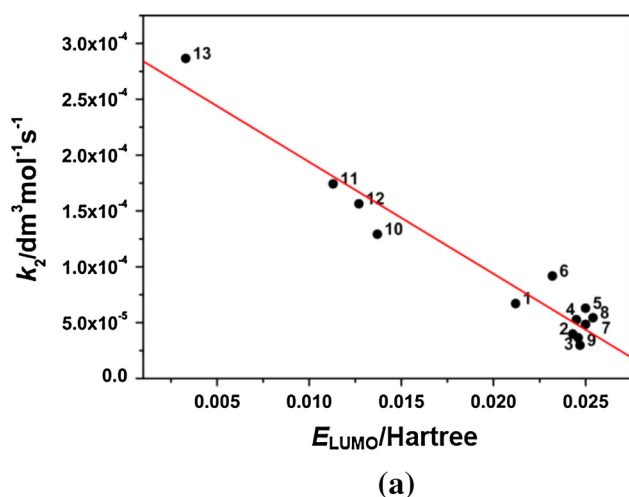
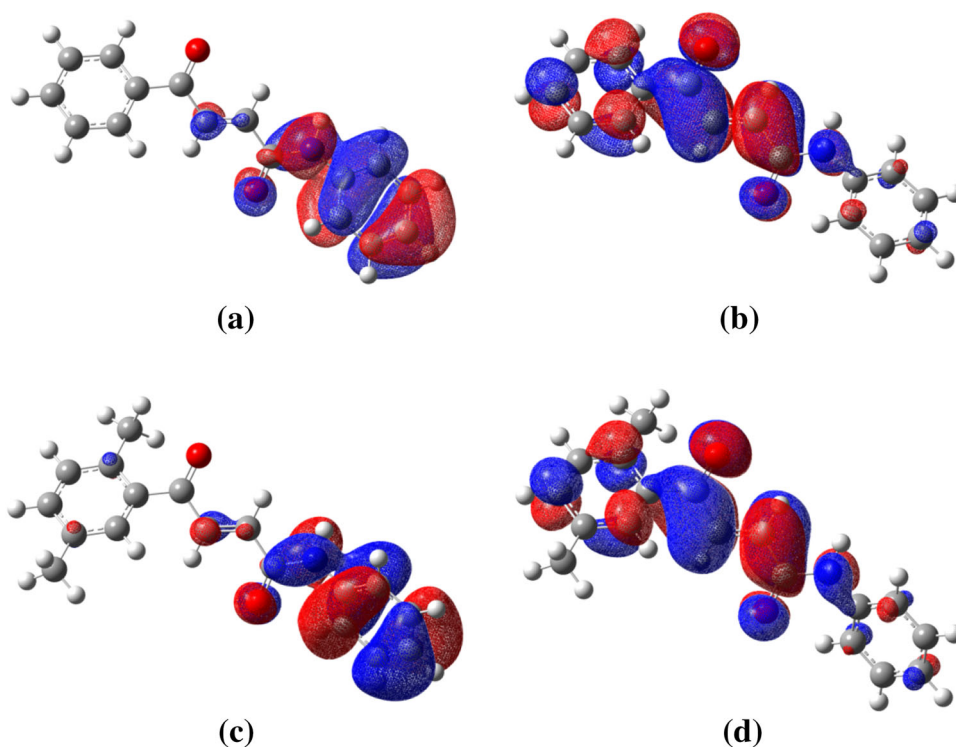


Fig. 4 Correlation between k_2 and energies of LUMO orbitals, obtained by MP2 calculations in vacuo, for the addition of: **a** piperidine, $r = 0.971$, $n = 13$, $F = 178.3$, slope = $-1.001 \times$

10^{-2} , intercept = 2.94×10^{-4} ; **b** benzylamine, $r = 0.976$, $n = 13$, $F = 218.3$, slope = -5.44×10^{-3} , intercept = 1.73×10^{-4}

spectrum of each adduct, the spatial vicinity of the aromatic hydrogen in *ortho*-position of aroyl moiety and AB protons of ABX pattern ($\text{ArC(O)-CH}_2\text{-CHR-C(O)NH-Ph}$) are clearly visible (Fig. 5).

Spatial vicinity of amido hydrogen ($-\text{NH}-$) and the X proton of the ABX moiety is also observed (Fig. S8 in Supplementary Material). This confirms that title compounds in aza-Michael additions act exclusively as unsaturated ketones, not as unsaturated amides.

Calculated UV/Vis spectra of the representative compounds

Progress of the addition of the piperidine and benzylamine to title compounds was monitored by UV/Vis spectroscopy. We calculated the UV/Vis spectra of representative compounds: unsubstituted derivative **1**, derivative having *ortho*-alkyl substituent **6**, and their adducts with piperidine and benzylamine (**1a** and **6a**), and compared calculated

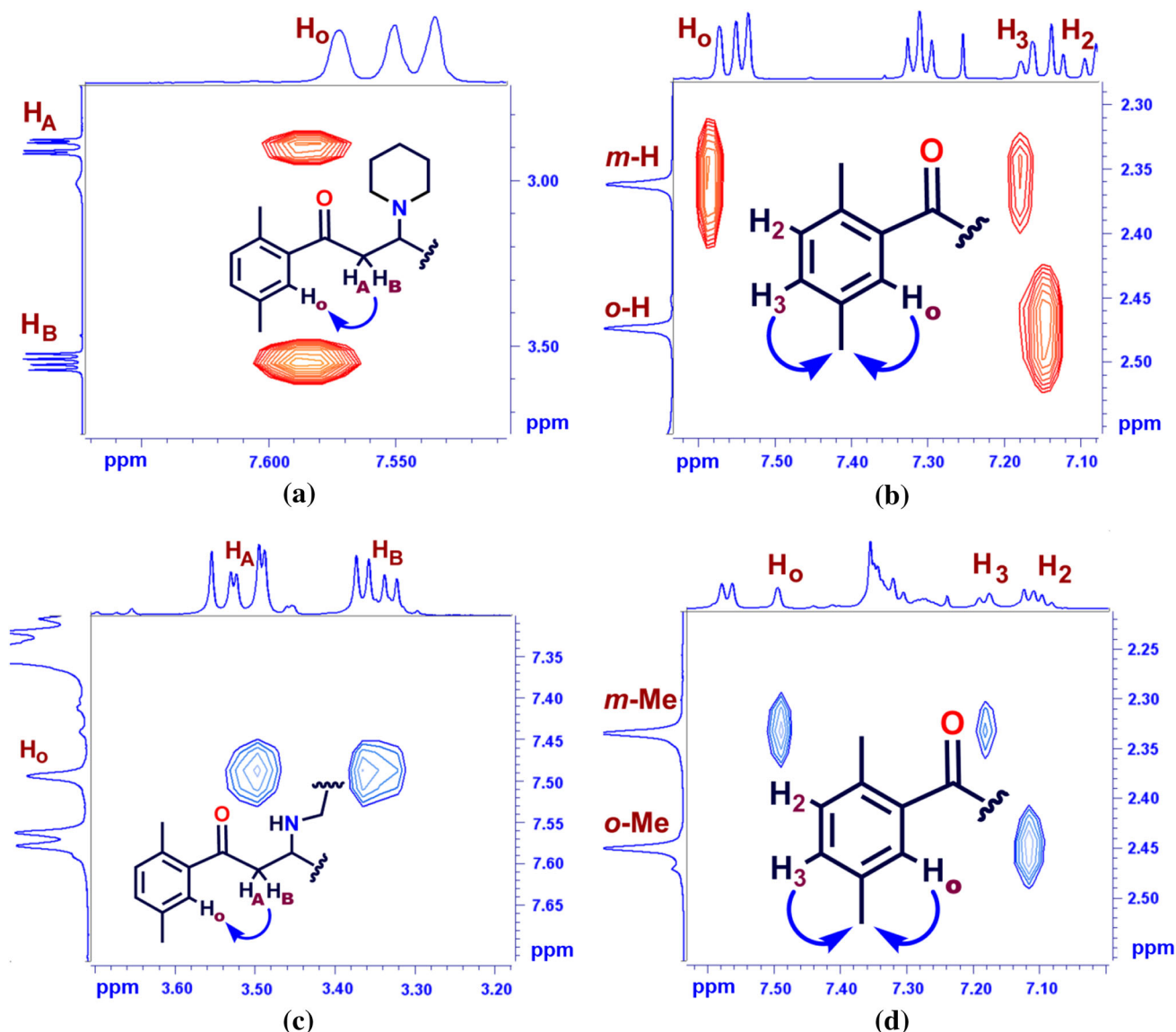


Fig. 5 **a** Section of the NOESY spectrum of the adduct of piperidine to compound **6** that shows spatial vicinity of the *ortho*-H on the 2,5-di-Me-phenyl moiety and AB protons of ABX pattern. **b** Position of *ortho*-H of aroyl moiety in the same compound. **c** Section of the

NOESY spectrum of the adduct of benzylamine to compound **6** that shows spatial vicinity of *ortho*-H on the 2,5-di-Me-phenyl moiety and AB protons of ABX pattern. **d** Position of *ortho*-H of aroyl moiety in the same compound

spectra with experimentally obtained ones. UV/Vis spectra were calculated using ZINDO/S, single-excitation CI (CIS, HF/6-311g), and TD-DFT (B3LYP/6-311g) methods, applying the implicit solvent model. Although not in full accordance with experimental data, ZINDO/S calculated spectra are most similar to experimentally obtained ones, except for compound **1a** (Fig. 6). For this compound, TD-DFT method provided a spectrum in fair agreement with experiments.

In Fig. 6, experimentally obtained spectra and spectra calculated by ZINDO/S method of compounds **1**, **6**, **1a**, and **6a**, are shown. Energies of HOMO and LUMO orbitals and

dipoles of compounds **1**, **6**, **1a**, and **6a** in excited states, obtained by ZINDO/S calculations, are shown in Table 3. For comparison, energies of HOMO and LUMO orbitals and dipoles for compounds **1**, **6**, **1a**, and **6a** calculated in ground states by MP2 method, with applied implicit solvent model, are shown in Table 2. In the calculated spectra, UV/Vis absorption maxima of compounds **1** and **6** at ~ 230 nm are blue-shifted for approx. 20 nm (Fig. 6a, b). In the UV/Vis spectrum of compound **1a** calculated by ZINDO/S method, the absorption maximum at ~ 270 nm appears, which does not exist in the experimental spectrum (Fig. 6c).

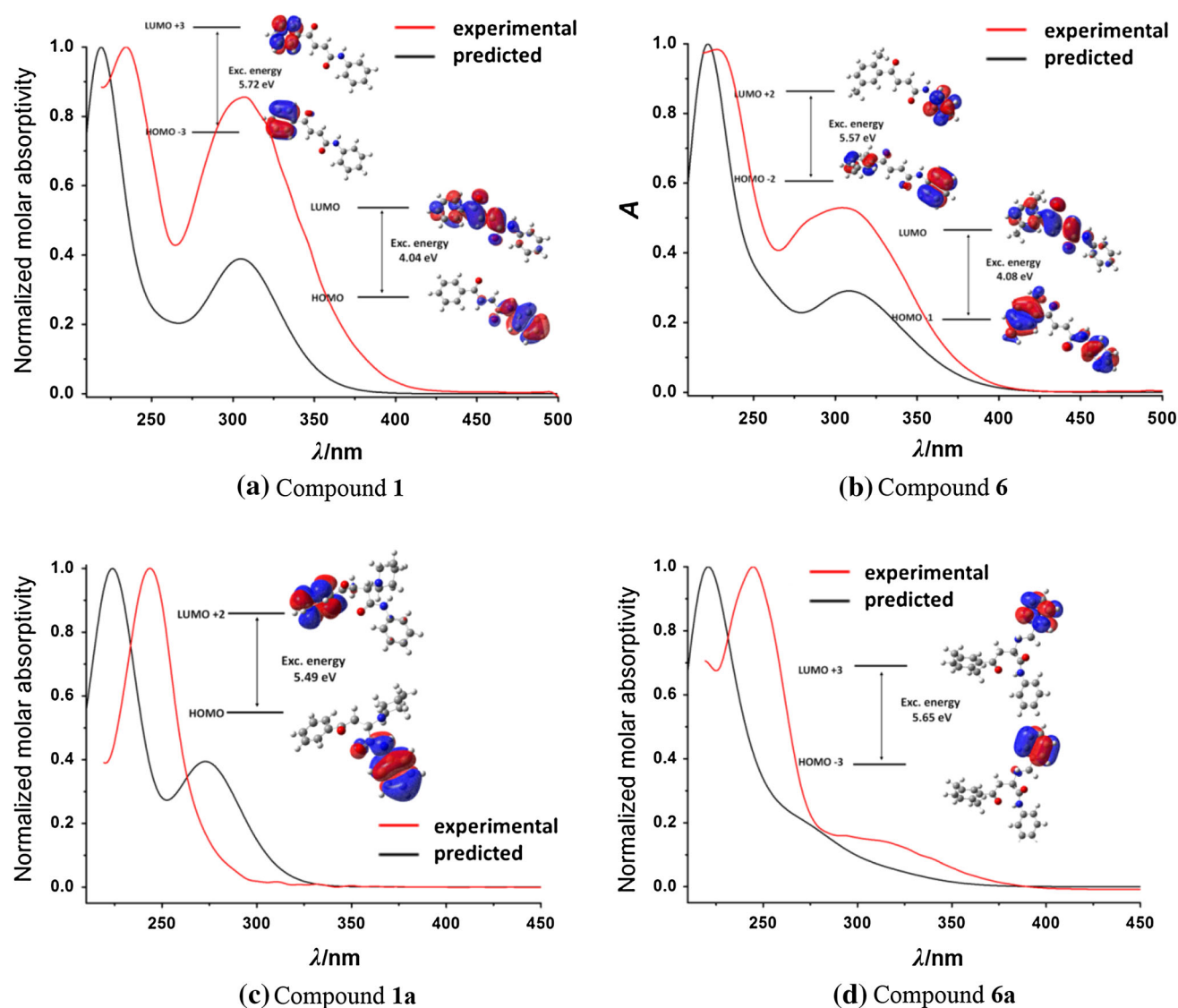


Fig. 6 Experimental and calculated UV/Vis spectra of: **a** compound **1**; **b** compound **6**; **c** compound **1a**; **d** compound **6a**. Molecular orbitals with the highest contribution to transitions associated with the two absorption

maxima (at ~ 220 and ~ 310 nm, for compounds **1** and **6**), or the one at ~ 220 nm (for compounds **1a** and **6a**) are depicted. Excitation energies, as obtained by ZINDO/S calculations, are also shown

Table 3 Energies of HOMO and LUMO orbitals and dipole moments of compounds **1**, **6**, **1a**, and **6a**

Comp. N°	$E_{\text{HOMO}}/\text{Hartree}$	$E_{\text{LUMO}}/\text{Hartree}$	μ/Debye
1	-0.31805	-0.05586	1.023
6	-0.31737	-0.05514	1.461
1a	-0.31378	-0.01898	1.544
6a	-0.31738	-0.02224	6.067

Data were obtained by the ZINDO/S method. Implicit solvent model was used in all calculations

The main contributions to the peaks in UV/Vis spectra at 305 and 308 nm of derivatives **1** and **6**, respectively, originate from HOMO to LUMO (Fig. 6a) and HOMO –

1 to LUMO transitions (Fig. 6b); while (calculated) peaks at 219 and 222 nm originate from HOMO – 3 to LUMO + 3 (Fig. 6a) and HOMO – 2 to LUMO – 2 transitions (Fig. 6b).

Results obtained from calculations are in accordance with the chemical intuition. Transitions originated by excitation from the HOMO to LUMO in a highly conjugate system ($\text{Ar-C(O)CH=CH-C(O)NH-Ph}$) causes an absorption peak at ~ 310 nm, while the absorption peak at ~ 220 nm involved the more localized aryl part of the molecules.

After Michael addition of amines, extensive conjugation is broken, so one absorption band at $\sim 245/220$ nm in experimentally obtained UV/Vis spectra of compounds **1a**

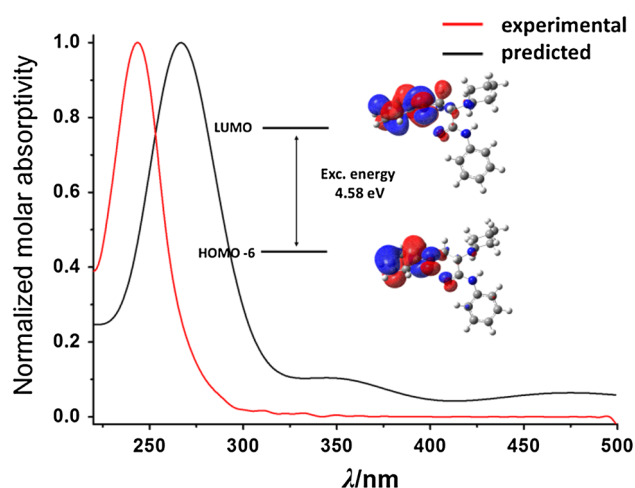


Fig. 7 Experimental and TD-DFT calculated UV/Vis spectrum of compound **1a**. Molecular orbitals with the highest contribution to transitions associated with the absorption maximum are depicted. Excitation energy, as obtained by TD-DFT calculations, is also shown

and **6a**, respectively, can be ascribed to transitions associated with the localized moiety of molecule.

Since the ZINDO/S method was unable to predict spectrum of **1a** with sufficient accuracy, we used CIS and TD-DFT calculations in order to obtain spectrum in better agreement with the experimental one. The spectrum most similar to the experimental one was obtained with TD-DFT calculations (Fig. 7). The one absorption maximum is predicted, red-shifted for ~ 30 nm compared to the experimentally obtained spectrum.

It should be noted that the position of the absorption maximum in the UV/Vis spectra of compound **1a** at ~ 270 nm calculated for the diverse set of conformers vary within 8 nm (data not shown).

In derivative **6a**, the main contribution to the absorption peak at ~ 220 nm arises from the transition associated with the benzylamino moiety of the compound (from HOMO - 3 to LUMO + 3, Fig. 6d).

Along with orbitals shown in Fig. 6, all molecular orbitals with significant contribution to the UV/Vis transitions of compounds **1**, **6**, **1a**, and **6a** are shown in Supplementary Material, Fig. S9, S10, S11 and S12.

Conclusions

The influence of phenyl ring substituents on the rate of addition of piperidine and benzylamine to (*E*)-4-aryl-4-oxo-2-butenic acid phenylamides was examined by measuring the rate constants. Rate constants for the addition of piperidine to compounds **1–13** were higher than the rate constants for the addition of benzylamine, but 10–100 times lower than the rates of the thia-Michael addition

obtained with 2-mercaptoethanol. Good correlations of the rate constants with the Hammett substituent constants, and with the atomic charges of the carbon atom in β -position of the aryl moiety of molecules were obtained. In such calculations *ortho*-substituted derivatives appear as strong outliers. Best correlations were obtained between the rate constants and energy of LUMO orbitals, derived from calculations on the MP2 level of theory. These correlations include all congeners examined. The regioselectivity of addition was confirmed by 2D NMR spectra of the isolated products. Adducts of piperidine and benzylamine in β -position to the aryl moiety of compounds were obtained, confirming that title compounds act as unsaturated ketones. The UV/Vis spectra of representative derivatives calculated by the ZINDO/S method are in fair agreement with the experimental ones.

Experimental

Preparation and characterization of compounds **1–13** was previously described [1]. The same samples were used for kinetic measurements reported herein. Synthesis and characterization of the adduct of compound **1** with piperidine (compound **1a**) was described previously [2]. UV/Vis spectra of compounds **1–13** and their adducts with piperidine and benzylamine were recorded in MeOH (p.a., Sigma-Aldrich) in concentrations of $\sim 1 \times 10^{-4}$ M, on a Cintra 40 UV/Vis spectrophotometer, thermostating the sample compartment at $25 (\pm 1)^\circ\text{C}$. Quartz cuvettes with 4 cm^3 volume and 1 cm path length were used for UV/Vis spectroscopy. ^1H , ^{13}C NMR and NOESY spectra were recorded on a Bruker AVANCE instrument at 500/125 MHz in CDCl_3 . Chemical shifts were reported in ppm relative to TMS. ESI-MS spectra were recorded on an Agilent Technologies 6210-1210 TOF-LC-ESI-MS instrument.

(*R,S*)-2-(Benzylamino)-4-(2,5-dimethylphenyl)-4-oxo-*N*-phenylbutanamide (**6a**, $\text{C}_{25}\text{H}_{26}\text{N}_2\text{O}_2$)

In a solution of 125 mg of (*E*)-4-(2,5-dimethylphenyl)-4-oxo-*N*-phenyl-2-butenamide (**6**, 4.47×10^{-4} mol) in 10 cm^3 of CH_3OH , a mixture of 92.6 mg of benzylamine (2 eq, 8.94×10^{-4} mol, 94.5 mm^3) and 95.4 mg of Na_2CO_3 (2 eq, 8.94×10^{-4} mol) were added and stirred for 2 h in round-bottom flask at room temperature. Afterward, the volume of solvent was decreased to about 1/10 of the initial under reduced pressure. Then 10 cm^3 of hexane/ Et_2O mixture (approximately 4:1) was added and flask was gently warmed for 5 min. The mixture was first cooled to room temperature and then placed in a refrigerator overnight. White precipitate was collected on a Büchner funnel

and washed with few drops of Et₂O, then dried in air. Yield: 96.5 %; white solid; m.p.: 82–83 °C (Et₂O/hexane); ¹H NMR (CDCl₃, 500 MHz): δ = 9.54 (s, 1H), 7.57 (d, *J* = 7.9 Hz, 2H), 7.49 (s, 1H), 7.33–7.36 (m, 4H), 7.31 (d, *J* = 7.9 Hz, 2H), 7.27 (t, b, 1H), 7.18 (d, *J* = 7.9 Hz, 1H), 7.08–7.12 (m, 2H), 3.93 (d, *J* = 13.0 Hz, 1H), 3.83 (d, *J* = 12.7 Hz, 1H), 3.77 (dd, *J*_{1,2} = 3.8 Hz, *J*_{1,3} = 7.5, 1H), 3.50 (dd, *J*_{1,2} = 3.4 Hz, *J*_{1,3} = 17.5 Hz, 1H), 3.34 (dd, *J*_{1,2} = 7.5 Hz, *J*_{1,3} = 17.5 Hz, 1H), 2.45 (s, 3H), 2.34 (s, 3H) ppm; ¹³C NMR (CDCl₃, 125 MHz): δ = 202.4, 171.6, 139.3, 137.7, 136.7, 135.4, 132.7, 132.0, 129.6, 129.0, 128.7, 128.1, 127.5, 124.1, 119.3, 59.1, 52.5, 42.4, 21.1, 20.8 ppm; HR/MS: calc for C₂₅H₂₆N₂O₂ (M + H⁺) 387.20670, found 387.20584.

Modeling

The values of Hammett substituent constants used in correlations were adopted from the literature [19, 20]. Cumulative substituent constants were used for compounds **5** and **13**. Nucleophilicity parameters *N* for piperidine and benzylamine are adopted from H. Mayr's 'Database of Nucleophilicities and Electrophilicities' [21]; using the data experimentally obtained in CH₃OH/CH₃CN (91/9) mixture [14], with the experimental setup closest to the experimental conditions used in this work. Initial geometries of compounds **1–13**, **1a**, and **6a** were obtained from SMILES notation in OMEGA [22, 23], as global minima with MMFF94s force field. The full geometry optimization was done in the Gaussian03 program [24] on the MP2 level of theory, using the 6-311G basis set, and tight criteria for self-consistent field convergence (SCF = tight keyword). The optimization of the (intermediate) geometries of compounds **1a** and **6a** on a semiempirical level of theory was done by the PM6 method [25] in MOPAC2012 [26, 27], using the implicit solvent model (COSMO). The UV/Vis spectra of compound **1**, **6**, **1a**, and **6a** were calculated from geometries found as the global minima on MP2 level of theory, by the semiempirical ZINDO/S method [28], using the implicit solvent model (polarizable continuum model, PCM—methanol). Time-dependent density functional (B3LYP/6-311g) and ZINDO/S calculations were performed in Gaussian09. All molecular orbitals are depicted on isovalue of 0.02 electrons/Å³.

Rate constants determination

Rate constants of the addition of piperidine and benzylamine to compounds **1–13** were obtained spectrophotometrically, under the pseudo-first order conditions, by measuring the decrease of absorbance at ~310 nm. Time scan measurements were carried out recording the absorbance in regular intervals (1 s), during the maximum of 20 min. Around

2.5×10^{-5} mol of **1–10** were dissolved in methanol in volumetric flask of 10.00 cm³ to obtain stock solutions. Around 1×10^{-5} mol of **11–13** were used because of limited solubility of compounds in MeOH. Aliquots ($\sim 2 \times 10^{-7}$ mol) of stock solutions of **1–13** were added in a quartz cuvette with the automatic pipette, and then 20-fold molar excess of deprotonated amine (C₅H₁₀N:⁻ or BzNH:⁻) in methanol (*c* = 0.02 M) was added. Deprotonated amines were prepared by the addition of stoichiometric equivalent of strong base, KOH, dissolved in MeOH. Pseudo first order rate constants (*k'*) were calculated by linearization of time scan plots, Eq. (2):

$$\ln \left(\frac{A_t - A_0}{A_\infty - A_0} \right) = -k' \cdot t, \quad (2)$$

where *A_t* is an absorbance of the solution in the time *t*, *A_∞* is the absorbance after completing of the reaction, and *A₀* is the initial absorbance. The *k'* was obtained as a mean from six independent measurements, using the same molar excess of amines. Second order rate constants were obtained by dividing *k'* with an amine/investigated compound molar ratio.

Acknowledgments The Ministry of Education, Science and Technological Development of Serbia support this work under Grant 172035. Authors gratefully acknowledge OpenEye Scientific Software, Santa Fe, NM, for the free academic licensing of software tools. The work reported makes use of results produced by the High-Performance Computing Infrastructure for South East Europe's Research Communities (HP-SEE), a project co-funded by the European Commission (under Contract Number 261499) through the Seventh Framework Programme HP-SEE (<http://www.hp-see.eu/>). Authors gratefully acknowledge computational time provided on the PARADOX cluster at the Scientific Computing Laboratory of the Institute of Physics Belgrade (SCL-IPB), supported in part by the Serbian Ministry of Education, Science and Technological Development under projects No. ON171017 and III43007, and by the European Commission under FP7 projects PRACE-3IP and EGI-InSPIRE.

References

- Vitorović-Todorović MD, Erić-Nikolić A, Kolundžija B, Hamel E, Ristić S, Juranić IO, Drakulić BJ (2013) Eur J Med Chem 62:40
- Vitorović-Todorović MD, Juranić IO, Mandić LJ, Drakulić BJ (2010) Bioorg Med Chem 18:1181
- Cvijetić IN, Vitorović-Todorović MD, Juranić IO, Drakulić BJ (2013) Monatsh Chem 144:1815
- Heintz W, Sokoloff N, Latschinoff P (1874) Ber Dtsch Chem Ges 7:1518
- Juaristi E, Soloshonok VA (2005) Enantioselective synthesis of β-amino acids, 2nd edn. Wiley, Hoboken
- Magriotis PA (2001) Angew Chem 113:4507
- Magriotis PA (2001) Angew Chem Int Ed 40:4377
- Rulev AY (2011) Russ Chem Rev 80:197
- Enders D, Wang C, Liebich JX (2009) Chem Eur J 15:11058
- Roberts DW, Franginal R, Lepoittevin JP, Benezra C (1991) Arch Dermatol Res 283:387
- Bernasconi CF, Ruddat V (2002) J Am Chem Soc 124:14968

12. Wiczling P, Markuszewski MJ, Kaliszan R (2004) *Anal Chem* 76:3069
13. Mayr H, Ofial AR (2008) *J Phys Org Chem* 21:584
14. Phan TB, Breugst M, Mayr H (2006) *Angew Chem Int Ed* 45:3869
15. Jaffé HH (1953) *Chem Rev* 53:191
16. Portal CF, Bradley M (2006) *Anal Chem* 78:4931
17. Hammett LP (1937) *J Am Chem Soc* 59:96
18. Pardo L, Osman R, Weinstein H, Rabinowitz JR (1993) *J Am Chem Soc* 115:8263
19. Hansch C, Leo A, Hoekman D (1995) *Exploring QSAR, hydrophobic, electronic and steric constants*. American Chemical Society, Washington, DC
20. Hanch C, Leo A, Unger SH, Kim KH, Nikaitani D, Lein EJ (1973) *J Med Chem* 16:1207
21. <http://www.cup.uni-muenchen.de/oc/mayr/DBintro.html>
22. Hawkins PCD, Skillman AG, Warren GL, Ellingson BA, Stahl MT (2010) *J Chem Inf Model* 50:572
23. Hawkins PCD, Nicholls A (2012) *J Chem Inf Model* 52:2919; OMEGA v. 2.4.2, OpenEye Scientific Software, Santa Fe, NM. <http://www.eyesopen.com>
24. Frisch MJ, Trucks GW, Schlegel HB, Scuseria GE, Robb MA, Cheeseman JR, Montgomery JA, Vreven T Jr, Kudin KN, Burant JC, Millam JM, Iyengar SS, Tomasi J, Barone V, Mennucci B, Cossi M, Scalmani G, Rega N, Petersson GA, Nakatsuji H, Hada M, Ehara M, Toyota K, Fukuda R, Hasegawa J, Ishida M, Nakajima T, Honda Y, Kitao O, Nakai H, Klene M, Li X, Knox JE, Hratchian HP, Cross JB, Adamo C, Jaramillo J, Gomperts R, Stratmann RE, Yazyev O, Austin AJ, Cammi R, Pomelli C, Ochterski JW, Ayala PY, Morokuma K, Voth GA, Salvador P, Dannenberg JJ, Zakrzewski VG, Dapprich S, Daniels AD, Strain MC, Farkas O, Malick DK, Rabuck AD, Raghavachari K, Foresman JB, Ortiz JV, Cui Q, Baboul AG, Clifford S, Cio-slawski J, Stefanov BB, Liu G, Liashenko A, Piskorz P, Komaromi I, Martin RL, Fox DJ, Keith T, Al-Laham MA, Peng CY, Nanayakkara A, Challacombe M, Gill PMW, Johnson B, Chen W, Wong MW, Gonzalez C, Pople JA (2003, 2009) *Gaussian03/09, Revision C.02*. Gaussian, Inc., Pittsburgh, PA
25. Stewart JJP (2007) *J Mol Mod* 13:1173
26. Stewart JJP (1990) *J Comput Aid Mol Des* 4:1
27. Stewart JJP; MOPAC2012; Stewart Computational Chemistry, Colorado Springs, CO, USA. <http://OpenMOPAC.net>
28. Ridley JE, Zerner MC (1973) *Theor Chem Acc* 32:111